High Pulse Repetition Frequency Operation of Low-power short-pulse Plasma Thruster

IEPC-2015-81／ISTS-2015-b-81

Presented at Joint Conference of 30th International Symposium on Space Technology and Science
34th International Electric Propulsion Conference and 6th Nano-satellite Symposium,
Hyogo-Kobe, Japan
July 4 – 10, 2015

Yuki Nakamura[1] and Hideyuki Horisawa[2]
Department of Aeronautics and Astronautics, Tokai University, Hiratsuka, Kanagawa, 259-1207, Japan

Abstract: *In this study, characterization of high-repetition frequency operation of a gas-fed low-power short-pulse plasma thruster with an applied magnetic field was conducted. A typical pulse repetition frequency was 15 kpps (pulse per sec) with maximum voltage of 6.5 kV and pulse width of 900 ns. The thrust performances with various conditions (mass flow rate, pulse repetition frequency etc.) were evaluated with a thrust stand. From the results, the maximum thrust and efficiency were 0.16 mN and 12%, respectively, for the maximum discharge voltage of 6.5 kV with a pulse duration of 900 ns and discharge energy of 18 mJ/pulse.*

I. Introduction

Pulsed-plasma thrusters, PPTs, utilizing a solid propellant usually PTFE (Teflon®), have attracted a growing interest for their system simplicity and advantages on miniaturization and mass reduction for the use of attitude or orbit control thrusters for small-sized spacecrafts, despite their low efficiency [1-4]. In their operations, short pulse discharges with several-microsecond duration are induced across an exposed propellant surface between electrodes, vaporizing and ionizing the surface, and also inducing a pressure force. Then an interaction of the discharge current (tens of kA) and its self-induced magnetic field results as the electromagnetic force, or Lorentz force, acting on the plasma and inducing a directed plasma beam exhaust, or thrust. In this electromagnetic acceleration process, it is necessary to complete phase changes of the propellant, such as vaporization and ionization, and the electromagnetic acceleration at the same time within a short duration of a pulse discharge. Improvements of the thrust performance can be expected with shorter pulse duration cases, since it is capable of higher current per unit time or higher power input, namely higher thrust, and of reducing loads on electrodes. However, it is difficult to complete the process including the phase changes and electromagnetic acceleration simultaneously during the discharge pulse, because there is a delay in the phase change of the solid-propellant after the pulse discharge initiation. The surface of the propellant will continue to evaporate long after completion of the discharge pulse, providing mass that cannot experience acceleration to high speeds by the electromagnetic and gas dynamic forces. The various masses including low-speed macroparticles can have quite different velocities. Since the residual vapor or plasma from the late-time evaporation of the propellant surface remains in the discharge channel due to the delay after the pulse discharge completion, which cannot contribute significantly to the impulse bit, it has been difficult for the thruster of this type to improve this mass loss of the propellant and thrust efficiency [1-4].

In order to improve the mass loss and thrust efficiency of PPTs, utilization various propellants in various phases, such as gas [5], liquid [6], powder [7], and laser ablation plasma [8-10] fed to the thrusters were investigated.

[1]Graduate Student, Department of Aeronautics and Astronautics, Tokai University, gaia_gene@yahoo.co.jp
[2]Professer, Department of Aeronautics and Astronautics, Tokai University, hideyuki.horisawa@gmail.com

Studies on gas-fed PPTs have been conducted from the late 1950's. The research includes coaxial, parallel-plate, z-pinch and hybrid geometries using ambient fill or pulsed gas injection techniques with hydrogen, nitrogen, argon, and xenon propellants [5].

Until recently the gas-fed PPTs suffered from low propellant utilization efficiency due to the fact that the fastest available space-qualified gas valve with long enough life (> 10^7 pulses) has an open time not shorter than 1 ms. As the time to fill the discharge chamber is only the on the order of 0.1 ms, much of the propellant could not utilized effectively over the life of the device. Recent work has resulted in a complete solution [11,12] to this problem by using state-of-the-art pulse power technology raising the propellant utilization efficiency to well above 90%. This solution relies on using modern pulsed-power conditioning technology to adjust the period between pulses to a length very close to the time it takes for the cold injected gas to fill the thruster chamber. This typically corresponds to pulse frequencies of a few kHz during the burst [12]. Depending on the available bus power and mission requirements, sets of such pulses can be produced such that each lasts a period that is at least as long as the response of a space-qualified valve (e.g. 1 ms) thus making sure that practically all injected propellant is utilized.

In this study, to develop novel gas-fed pulse plasma thrusters, which can be operated in a continuous mode, discharge characteristics and plasma (electron and ions) acceleration characteristics of high-peak power short-pulse discharges were investigated. The acceleration regime of plasma through the interaction of short-pulse discharges with matter clearly differs from the conventional acceleration regimes. Recent rapid progress of pulse power generation technologies associated with recent development of power sources for photolithography of next-generation semiconductors has brought high-peak power sort-pulse drivers for extreme ultraviolet (EUV) and X-ray sources, particle accelerators, etc. With this regime, a wide range of plasma densities, or acceleration regimes, from electrostatic acceleration to electromagnetic acceleration, can be expected, namely achieving either high-specific impulse accelerator or high-impulse accelerator depending on the mission requirement, which can possibly realize a highly robust propulsion system for future spacecraft. The primary objective of this study is to demonstrate these significant characteristics.

Authors have been investigating laser-assisted pulsed plasma thrusters (LAPPTs) and have demonstrated their high specific impulse characteristics [8,9]. In this study, as the next step, reducing discharge pulse width using newly developed pulse power source with higher repetition frequencies, high-repetition rate discharges were demonstrated and their characteristics were investigated.

II. Experimental setup

A. Rectangular gas-fed short-pulse plasma thruster with external magnetic field

In general, primary acceleration mechanisms of pulsed plasma thrusters include following two regimes, 1) electromagnetic acceleration regime, in which an interaction, or Lorentz force, between a pulsed discharge current and a self-induced magnetic field induced by the current accelerates plasma in the discharge channel, and 2) electro thermal acceleration regime, where plasma with high thermal energy, due to Joule heating by the discharge current, is expanded and accelerated aerodynamically. However, to achieve a high-repetition frequency of pulsed discharges, discharge energy, or current, per pulse should be limited due to the limited capability of a power source. In this case, because of the lower current, a self-induced magnetic field generated by the discharge current, will not be high enough. In our thruster, to enhance the magnetic field, an external magnetic field is applied in the acceleration channel.

Figure 1 shows an external view of a rectangular gas-fed short-pulse plasma thruster with external magnetic field using a permanent magnet developed in this study, and its cross-sectional view is illustrated in Fig.2. As shown in these figures, a rectangular acceleration channel consists of parallel electrodes made of tungsten rods (5 mm in length, 3 mm in diameter, gap of electrodes of 5 mm) and glass side-walls insulating yokes for a magnetic circuit from the electrodes.

In the acceleration channel, an external magnetic field normal to a discharge current is applied as shown in Fig.1. As for a magnetic field source, a neodymium magnet is employed, and a magnetic circuit consisting of soft steel yokes is designed to generate a strong magnetic field in the acceleration channel. A typical magnetic field distribution of applied to the acceleration channel obtained from FEM simulation is shown in Fig.3. This figure is a top view of the thruster, and then a horizontal component distribution of magnetic field is visualized. From the figure, it is shown that the maximum magnetic field strength is 1.48 T in the center of the acceleration channel. As for the propellant in this study, argon gas is employed. Although the discharges are in repetitively pulsed operation, argon gas is continuously fed to the acceleration channel.

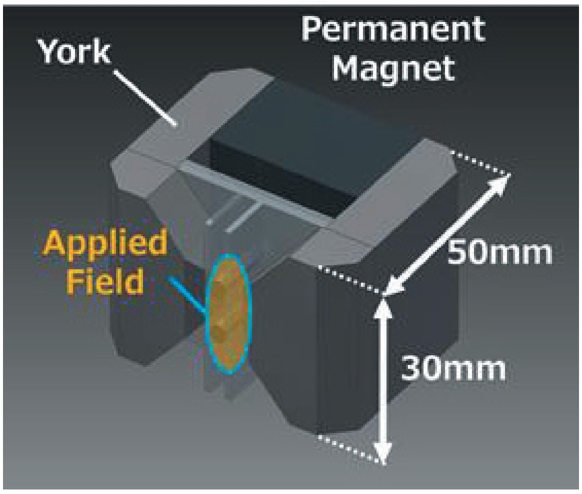

Fig.1 A rectangular gas-fed short-pulse plasma thruster with external magnetic field using permanent magnet.

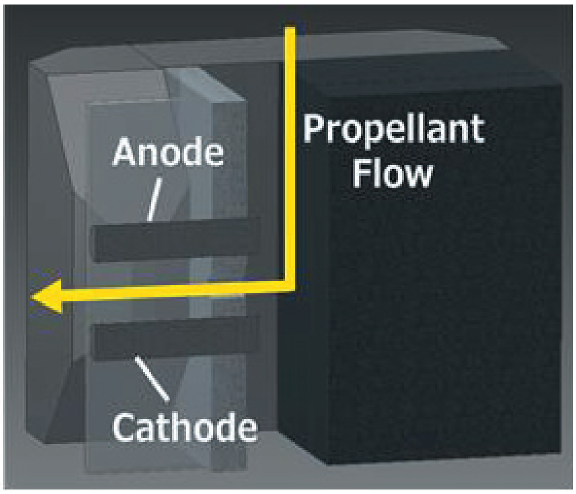

Fig.2 Cross-sectional view of thruster.

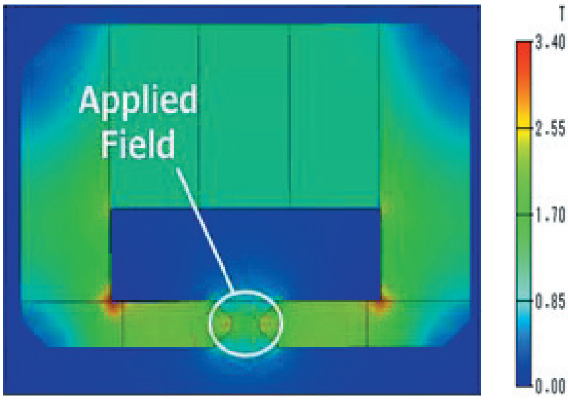

Fig.3 Magnetic field distribution of applied magnetic field of thruster obtained from FEM simulation.

B. Short-pulse power source and thrust stand

A schematic of experimental setup is illustrated in Fig.4. Trains of pulse waves are generated by a function generator (FG-350, Iwatsu Test Instruments Corporation), and amplified by a power amplifier (NF4505, NF Corporation, average output power of 350 W). Then after boosted by a transformer (Union Electronics), high-voltage repetitive pulse discharges are generated.

Typical repetition rates of the pulse discharges are 10 ~ 19 kpps with the maximum voltage of 3.5 kV and pulse duration of 900 ns (FWHM)

As shown in this figure, thrust measurement is conducted with a thrust stand installed in a vacuum chamber. As for the argon gas propellant, typical mass flow rates are 5 ~ 10 sccm. In the maximum propellant flow case, the internal pressure of the vacuum chamber can be maintained below 5 x 10-3 Pa. A thrust stand developed and used for the measurement is shown in Fig.5. A height of the thrust stand made of stainless steel is 400 mm and a length of a pendulum arm is 300 mm. A knife edge is employed for the pivot. As shown in the Figs.4 and 5, the thruster is hung at the lower edge of the pendulum. With the thruster installed on the pendulum, a natural period of the pendulum is about 1 s. When the thruster is in operation, a horizontal displacement the pendulum is induced by the thrust, and then by measuring the displacement, a thrust is estimated.

To measure the displacement, a laser displacement sensor is employed (KEYENCE LK-01, minimum resolution of 20 um). Although this thruster generates repetitive pulsed discharges, the facts, that a pulse duration of 400 ns is significantly smaller than a natural period 1 s of the pendulum and that a typical repetition rate of 10 kHz is much larger than a natural frequency of the pendulum 1 Hz, allows us to assume the thrust acting on the pendulum is regarded as a steady force. Before each thrust measurement, calibration of the stand was conducted. From the calibration, the minimum resolution of the thrust was about 100 nN.

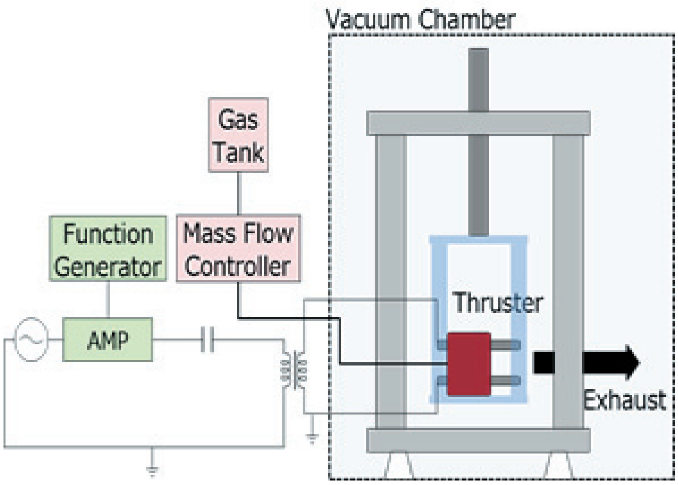

Fig.4 Schematic of experimental setup.


Fig.5 Photo of thrust stand.

C. Calibration of thrust stand

Since a small thrust could be expected by a cold gas jet estimated as high as 20μN, the calibration of the thrust stand should range from 2 μN to 0.1 mN. Because the lower range is very small to calibrate, the calibration range, or namely method, was divided into two ranges (first range: 2 ~ 10μN, second range: 10μN ~ 0.1 mN).

Although arbitrary weights can be used for the larger (second) range of the thrust, the weights are not easily applicable for much smaller forces (first range). Because of this difficulty with the weights, an electrostatic actuator was employed for the calibration of the first range. A schematic of calibration setup using arbitrary weights for the second (larger) range is shown in Fig.6. As shown in this figure, a mass of a weight can generate an arbitrary force, or namely a displacement, on the pendulum in this system. The weights are made of copper with the masses of 2 ~ 10 mg. A thin nylon string of less than 0.1 mg was employed to connect the mass and pendulum.

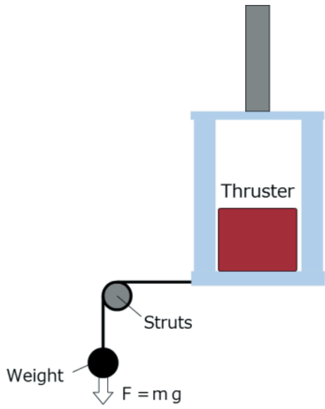

Fig.6 Calibration of thrust stand with arbitrary weights.

A schematic of calibration setup using an electrostatic actuator for the first (smaller) range is shown in Fig.7.

As shown in this figure, an arbitrary electrostatic force is induced when an arbitrary voltage is applied to a pair of planer plates with arbitrary gaps, and then a displacement of the pendulum will be induced.

The applied voltage was fixed as 320 V. The gap between the plates was adjusted with a linear actuator enabling the gaps to be controlled from 1 ~ 2 mm, which were also monitored with a laser displacement sensor. A schematic of calibration setup using an electrostatic actuator for the first (smaller) range is shown in Fig.7.

As shown in this figure, an arbitrary electrostatic force is induced when an arbitrary voltage is applied to a pair of planer plates with arbitrary gaps, and then a displacement of the pendulum will be induced.

The applied voltage was fixed as 320 V. The gap between the plates was adjusted with a linear actuator enabling the gaps to be controlled from 1 ~ 2 mm, which were also monitored with a laser displacement sensor.

$$F = \frac{1}{2}\varepsilon_0 \left\{ \left(a + \frac{3}{8}D\right)\left(b + \frac{3}{8}D\right) \right\} \frac{V^2}{D^2} \quad \cdot \cdot \cdot (1)$$

A relationship between a displacement, or a gap, and a force can be expressed by a gap D, area of plates S, and applied voltage V. Where, ε_0 is dielectric constant in vacuum, a and b are vertical and horizontal lengths of the plates ($S = a \times b$). In Eq. (1) an edge effect of plate edges is also included. Results of the calibration for two regions are plotted in Fig.8.

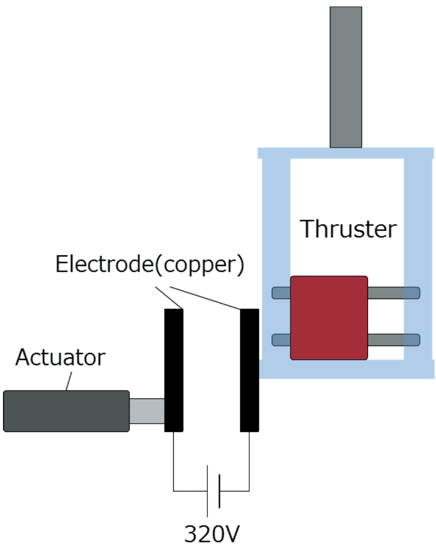

Fig.7 Calibration of thrust stand with electrostatic actuator.

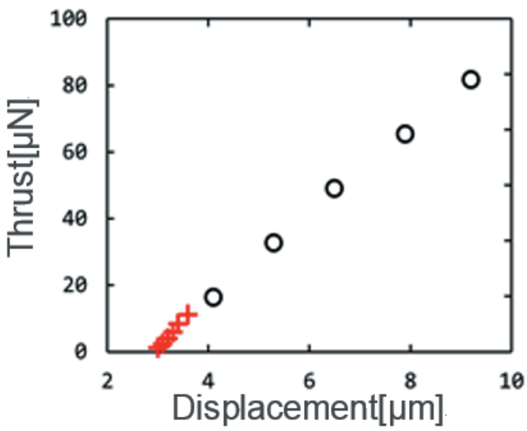

Fig.8 Results of calibrations.

III. Results and discussion

A typical discharge voltage waveform is shown in Fig.9. It is shown that the maximum voltage is 6.5 kV with a pulse duration of about 900 ns in this case. Effects of repetition rates on thrust and thrust efficiency, respectively, are plotted in Figs.10 and 11. In the figures, it can be seen that thrust and efficiency increase with repetition rates of pulses and mass flow of the propellant. The maximum thrust and efficiency are 0.16 mN and 12%, respectively at mass flow of 10 sccm and repetition rate of 19 kpps.

Since average input powers for these experiments were about the same, an energy per pulse must be reduced at higher repetition rate cases. Typical discharge energies for each pulse were 35 mJ/pulse for 10 kpps, 23 mJ/pulse for 15 kpps, and 18 mJ/pulse for 19 kpps.

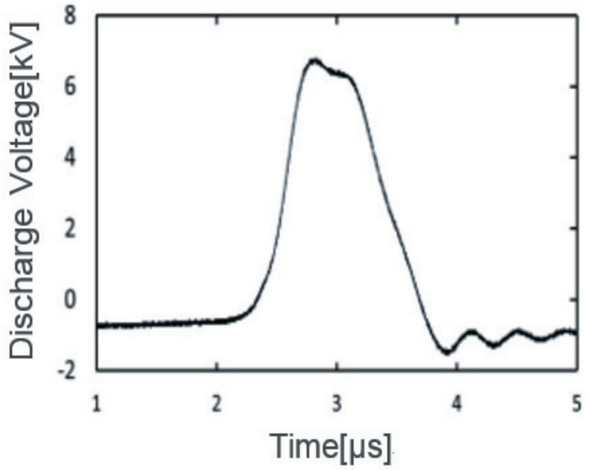

Fig.9 Typical discharge voltage waveform.

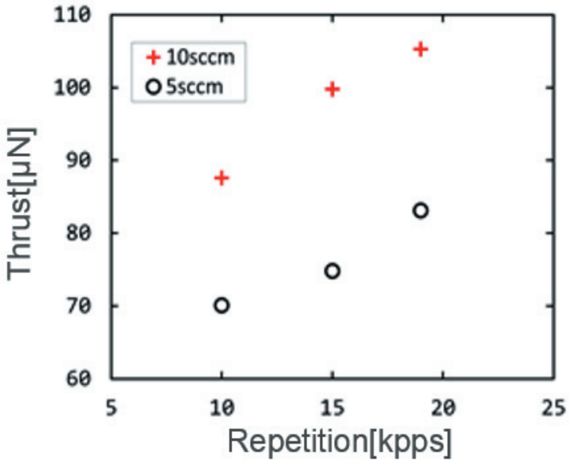

Fig.10 Effect of repetition rates on thrust.

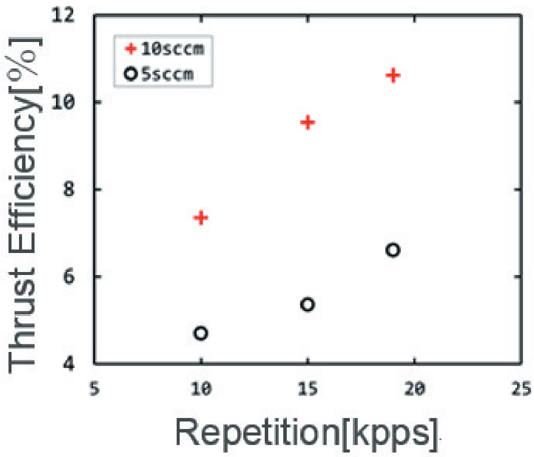

Fig.11 Effect of repetition rates on thrust efficiency.

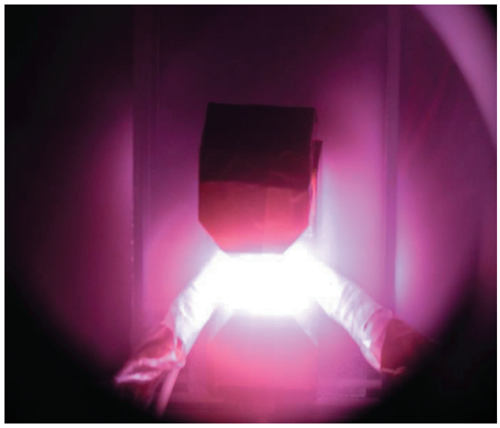

Fig.12 Photo of ignition experiment

IV. CONCLUSION

In this study, characterization of high-repetition frequency operation of a gas-fed low-power short-pulse plasma thruster with an applied magnetic field was conducted. A typical pulse repetition frequency was 15 kpps (pulse per sec) with maximum voltage of 6.5 kV and pulse width of 900 ns. Results obtained in this study are as follows.

1) The maximum thrust and efficiency were 0.16 mN and 12%, respectively.
2) The maximum discharge voltage was 6.5 kV with a pulse duration of 900 ns.
3) A typical discharge energy was 18 mJ/pulse in the case of maximum thrust efficiency.

Currently, development of power sources with higher repetition rates and shorter pulse durations is conducted to investigate the influences of these parameters on the thrust performance .

Reference

1. Jahn, R.G., Physics of Electric Propulsion: McGraw-Hill, 1968, pp.198-316.
2. Martinez-Sanchez, M., and Pollard, J. E., J. Propulsion and Power 14, pp.688-699 (1998).
3. Burton, R. L., and Turchi, P. J., J. Propulsion and Power 14, pp.716-699 (1998).
4. Micci, M. M., and Ketsdever, A. D. (ed.), Micropropulsion for Small Spacecraft (Prog. Astronautics and Aeronautics 187): American Institute of Aeronautics and Astronautics, 2000, pp.337-377.

5 Ziemer, J., Performance Scaling of Gas-Fed Pulsed Plasma Thrusters, PhD Dissertation, Princeton U (2001)

6. Kakami, A. Koizumi, H., Komurasaki, K. Arakawa, Y., ISTS2002-b-15（2002）
7. Yokoyama, S., Horisawa, H. Funaki, I., Kuninaka, H., "Fundamental Experiment of Laser Micro Propulsion using Powdered-Propellant", ISTS 2006-s-10, 2006.
8. Horisawa, H., et al., Applied Physics A 81 (2005)
9. Kishida, Y., et al., Trans. JSASS 8 (2010)
10. Y. Oigawa, et.al., AIAA-2014-3537（2014）
11. Ziemer, J. K., Cubbin, E. A. Choueiri, E. Y., Birx, D., "Performance characterization of a high efficiency gas-fed pulsed plasma thruster", AIAA 97-2925, 1997.
12. Ziemer, J. K., Choueiri, E. Y, Birx, D.,"Is the Gas-Fed PPT an Electromagnetic Accelerator? An Investigation using Measured Performance", AIAA-99-2289, 1999.